Comparative Sensibility Study of WO₃ ph Sensor Using EGFET and Ciclic Voltammetry

Renata de Castro Campos[a], Dane Tadeu Cestarolli[a], Marcelo Mulato[b], Elidia Maria Guerra[a]*

[a]Departamento de Química, Biotecnologia e Engenharia de Bioprocessos – DQBIO, Universidade Federal de São João del-Rei – UFSJ, Rod. MG 443, Km 07, CEP 36420-000, Ouro Branco, MG, Brazil
[b]Departamento de Física – DF, Faculdade de Filosofia, Ciências e Letras de Ribeirão Preto – FFCLRP, Universidade de São Paulo – USP, Av. Bandeirantes, 3900, CEP 14040-901, Ribeirão Preto, SP, Brazil

In this present study, the investigation about pH sensorial properties of WO_3, via sol-gel, was evaluated by Voltammetry and Extended Gate Field Effect Transistor techniques. The X-ray diffractogram indicates the presence of a lamellar structure, $d = 0.69$ nm, resulting in $WO_3.2H_2O$. From Scanning Electron Microscopy of $WO_3.2H_2O$ was observed a process corresponding to the delamination which consists of irregular stacking with rounded platelets. The $WO_3.2H_2O$ was investigated as a pH sensor in the pH range 2–12, by the EGFET and Voltametry techniques presenting a sensitivity of 52 mV/pH and 60 mV/pH, respectively. These results can indicate that both Voltammetry and EGFET techniques present values close to the theoretical limit (59.2 mV/pH) as well as the material is a promising candidate for applications as a pH sensor and as disposable biosensor in the future.

Keywords: *tungsten oxide, pH sensor, voltammetry, EGFET*

1. Introduction

The search for simple, speedy and inexpensive analytical tests utilizing chemical compounds at very low concentrations has caused a growing need for the development of electrochemical sensors[1,2]. For example, the biosensors on basis of the pH sensor are widely utilized in the medical instruments. In order to obtain an improvement in the sensitivity Bergveld proposed the Ion-Sensitive Field-Effect Transistor (ISFET)[3]. The development of the ISFET mimics a commercial Metal Oxide Semiconductor Field Transistor (MOSFET) in which the metal gate electrode is removed, in order to expose the underlying insulator layer to the solution. Based on ISFET, Van Der Spiegel et al.[4], introduced another structure named Extended Gate Field Effect Transistor (EGFET) which has a more flexible shape compared to ISFET, and also presents better long-term stability, since the ions from the chemical environment are excluded from any region close to the FET gate insulator[5]. Recently, several thin films have been widely used as the sensing material of the EGFET pH sensors, such as carbon nanotubes[6], SnO_2[7], ZnO[8], V_2O_5 xerogel[9], V_2O_5/HDA[10], V_2O_5/WO_3[11], V_2O_5/TiO_2[12,13].

However, the search for improved materials as an alternative for ion-sensing membranes still remains in this field of study. An alternative to ion-sensing membranes used in pH sensors is the tungsten oxide (WO_3) thin film obtained by the sol-gel route. WO_3 thin film presents the hopping conduction between W^{6+} and W^{5+} or W^{5+} and W^{4+} that may result in not only high conductivity but also high carrier mobility[14]. The conduction of WO_3 thin films is very anisotropic, and across the W–O–W layers it is proposed to be due to, mainly, protons which move through

hydrogen bonds[11]. Research on WO_3 thin films has generated significant interest because of their use in Semiconducting Metal Oxide (SMO)-based sensors for the detection of gaseous adsorbates[15] and because they are amenable to microfabrication techniques[16].

The aims of this work are to explore WO_3 thin films as ion-sensitive membranes with charges in pH solutions, to find out the sensor sensitivity, and to verify its suitability as a pH sensor. Finally, the used pH-sensor sensitivity should be verified and the results obtained for the EGFET and Voltammetry techniques should be compared.

2. Experimental

The tungsten oxide gel, $WO_3.nH_2O$, was prepared from sodium tungstate ($NaWO_3$, VETEC), by the ion exchange method (ion-exchange resin Dowex-50X8) as described in the literature[11]. Acid solutions were obtained by percolating 0.1M of $NaWO_3$ aqueous solutions through a cationic ion-exchange resin. Upon standing at room temperature (24 °C) for 2 weeks, the solutions were polymerized, leading to a viscous yellow gel of WO_3. The WO_3 gel was deposited on an indium tin oxide/polyethylene terephthalate (ITO/PET) substrate and dried at room temperature, leading to the formation of a thin film.

The X-Ray Diffraction (XRD) data were recorded on a SIEMENS D5005 diffractometer using a graphite monochromator and CuK_α emission line (1.541 Å, 40 kV, 40 mA). After that, samples in the film form deposited onto a glass plate were employed, and the data were collected at room temperature over the range $2° \le 2\theta \le 50°$, with a step of 0.020°.

*e-mail: elidiaguerra@ufsj.edu.br

Scanning Electron Microscopy (SEM) was carried out on a ZEISS microscope EVO 50 model operating at 20 kV. A thin gold coating (≈ 20Å) was applied to the sample using a Sputter Coater – Balzers SCD 050. The length of platelets particles was found using the software ImageTools®.

The electrical response of the sensor was measured using varying pH solutions, and the curves were obtained by an Agilent 34970A parameter analyzer. The electrode containing the film was dipped into the buffer solution, at room temperature, for 5 minutes, prior to the electrical measurement.

Voltammograms were measured using an AUTOLAB (Metrohm) model PGSTAT 302N (Nova 1.10) potentiostat/galvanostat interfaced with a computer. The conventional electrode arrangement was used, which consisted of PET/ITO as the working electrode, a platinum wire auxiliary electrode, and a saturated calomel electrode (SCE) as the reference. The WO_3 thin film was deposited on the electrode surface by evaporating approximately 5 ml of the suspension at room temperature (24 °C). The electrode containing the film was dipped into the buffer solution at room temperature, for 5 minutes, prior to the electrical measurement. The buffer solutions used as supporting electrolyte had pH = 2, 4, 6, 7, 8, 10 and 12 each one.

3. Results and Discussion

The X-ray diffraction pattern of a tungsten oxide is shown in Figure l. It exhibits series of harmonic peaks, that can be indexed as *0k0*, according to the $WO_3.nH_2O$[17]. Besides that, the *0k0* index corresponds to the stacking of platelike particles along a direction perpendicular to the substrate. Additionally, the peaks also indicate that the lamellar structure of the WO_3 is maintained after the drying process as observed in Figure 2. Based on Bragg's law, the basal spacing, *d*, between the platelets ($d = 0.69$ nm) suggests that water molecules (n = 2) are intercalated between these platelets resulting in $WO_3.2H_2O$, as also observed in the literature[17]. Despite of cristallinity, the diffraction peaks of the $WO_3.2H_2O$ present high intensity and narrow peaks suggesting that this material has a highly crystalline structure.
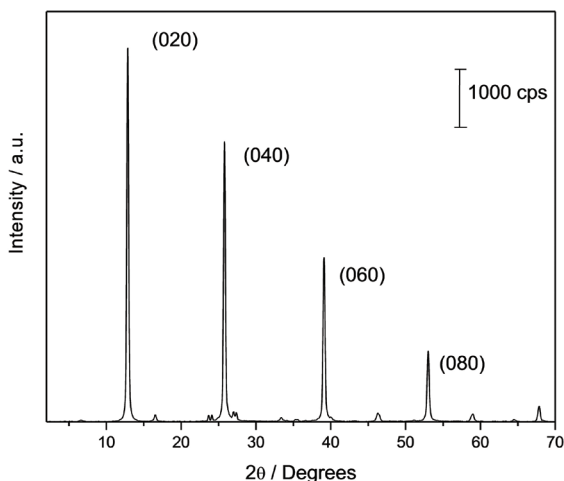
Figure 2 shows the scanning electron micrographs of the WO_3. In this image was observed a process corresponding to the delamination of the stacked inorganic sheets. The crystallites of the material consist of irregular stacking with rounded platelets with a length of around 10–20 nm and thickness less than 1.0 nm, consistent to what is showed in Figure 1.

Figure 3 shows the drain current (I_{DS}) as a function of the voltage between transistor gate and source (V_{GS}) for the WO_3, in contact with a buffer solution. It is observed that the threshold voltage shift depends upon the pH value, i.e., the threshold voltage shifts from the left to the right with increasing pH values. This dislocation towards higher voltages as a function of pH is due to the sensing properties that are associated to the potential-determining ions in the buffer solution (i.e., H^+ and OH^- ions). As the pH values of the buffer solution are increasing, there is a threshold voltage shift positively because of the decreasing surface potential. Based on this fact, the sensitivity of pH sensors can be extracted from the threshold voltage shift from Equation 1 and 2, i.e.[18],
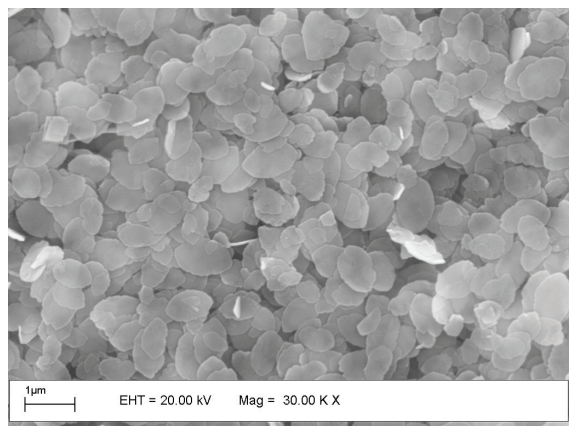

Figure 2. Scanning Electronic Microscopy of WO_3.
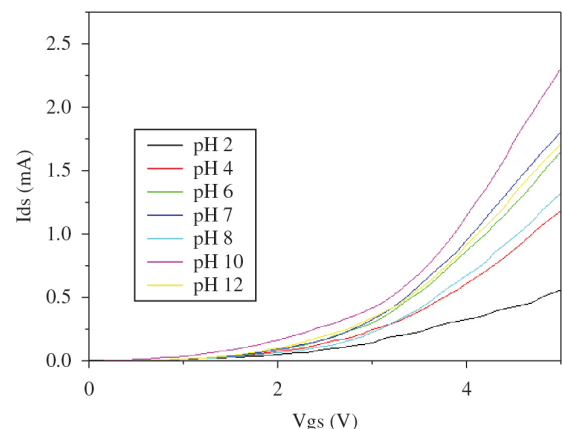

Figure 1. Diffractogram of sol-gel WO_3.

Figure 3. EGFET response in linear region (drain–source current as a function of gate–source voltage) using WO_3.

$$sensitivity = \frac{VT(EGFET) \times (pH') - VT(EGFET) \times (pH)}{pH' - pH} \quad (1)$$

$$= \frac{\Delta V_{T(EGFET)}}{\Delta pH} \quad (2)$$

From Figure 3, an I_{DS} value of 350 µA was adopted for determination of the sensitivity and the corresponding V_{GS} values were plotted as a function of the pH for all the samples (Figure 4). Based on the experimental results shown in Figure 3, the sensitivity of the EGFETs using $I_D = 350$ mA and V_{DS} of 0.3 V was 52 mV/pH. It is possible to note that the sensitivity is very close to the theoretical limit[19]. Besides that, Figure 4 shows that the EGFET exhibits good linearity.

The behavior of the voltammogram and its correlation with the pH response were also accompanied and it is showed in Figures 5 and 6. Each exchange of buffer solution to a higher pH can result in altering the concentration of one of the species involved in the reaction, thus resulting in a shift in the redox potential. Figures 5 and 6 show the voltammograms as a function of pH, in buffered electrolytes. It was used a sweep rate slow (20 mV/s) in order to ensure that the main features of the voltammogram were reversible. The anodic peak region was selected, in order to ensure that the main features were preserved and to facilitate voltammogram analyses. The equation for the electrode potential of this half-reaction can be rearranged. Figure 6 shows that the potential shifts to more negative values as the pH increases as predicted by the Nernst equation in Equation 3[20].

$$E = E1/2 - \frac{0.0592}{2} \log\frac{[H2Q]}{[Q]} - 0.0592 \times pH \quad (3)$$

The pH dependence of potential (E) can also be seen in Figure 7, where E is plotted against the pH. The slope of the line is 60 mV/pH. From the Nernst equation, the slope of the plot of E vs. pH should be 59.2 mV/pH, which is very close to the values obtained from the EGFET study.
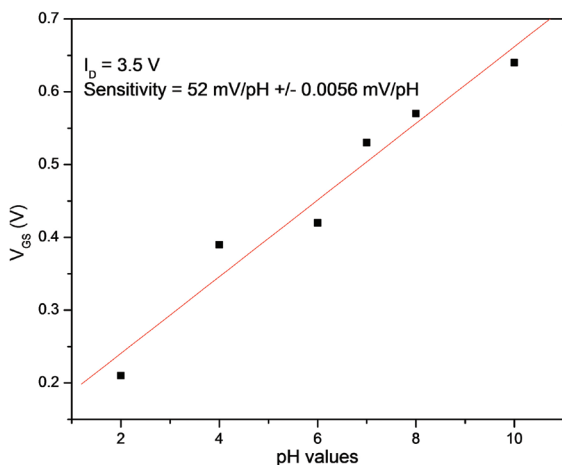
Therefore, the EGFET-pH sensor based on tungsten oxide is a promising method and it might be suitable to be used as a device in disposable sensors.

The sensorial capability occurs at the oxide/solution in both Voltammetry and EGFET analyses. When a potential
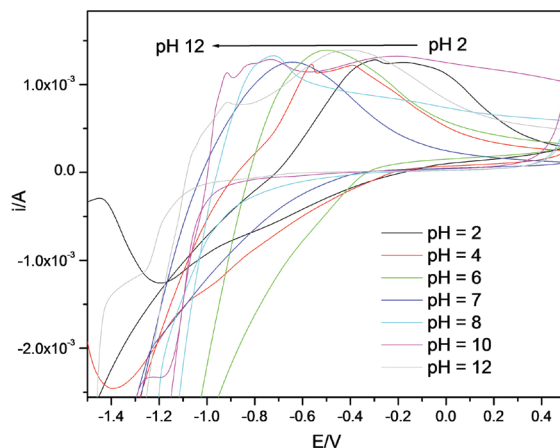
Figure 5. Voltammograms of WO$_3$ in buffer solution with pH values ranging from 2 to 12.
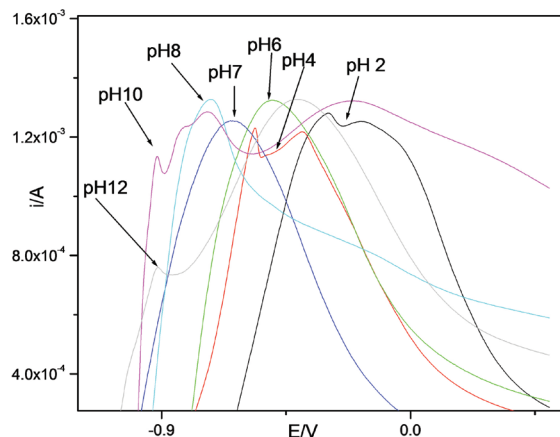
Figure 6. Voltammograms of WO$_3$ in buffer solution with pH values ranging from 2 to 12 with magnification to guide the eyes.

Figure 4. Sensitivity of the WO$_3$ EGFET pH sensor for buffer solutions with pH varying from 2 up to 10, for the linear region.
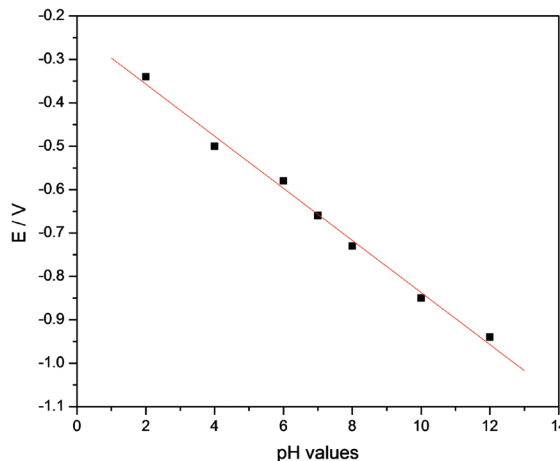
Figure 7. Potential range as a function of pH values for the WO$_3$.

is applied, charge may arise by the adsorption/desorption of H^+ ions in the interface modified in both sign and intensity, depending on the pH of the solution in contact with the sample. Thus, this charge assumes that the Nernst equation relates the total double layer potential drop to the activity in solution of H^+ (or OH^-) i.e. the potential-determining (p.d.) ions[21]. From this point of view, both the EGFET and voltammetric sensors exhibit the same electrochemical mechanism involving charged interfaces and binding sites of H^+ and OH^-. These sites can be protonated or deprotonated, leading to a surface charge which is dependent on the pH of the electrolyte, and controls the surface potential[9,22]. In the voltammetry is possible to sweep a pontential to the regions which the electroactive species exist as oxidized (Ox) as well as, followed to reduced species (Red) and when the ratio [Ox]/[Red] approaches to zero it is called isoelectric point or zero (IEP).

During the variation of pH values it was observed a occurrence of a protonation/deprotonation mechanism in the IEP that was previously described in the literature[13,23]. Based on the protonation/deprotonation mechanism, it is possible to consider that Reaction (1) in pH < IEP, pH = IEP and pH > IEP, respectively:

$$M - OH_2^+ \leftrightarrows M - OH + H^+ \leftrightarrows M - O^- + 2H^+ \qquad (1)$$
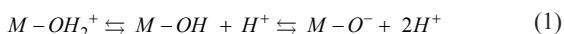
Based on the reaction 1, the voltammetric and EGFET studies, Figures 4 and 6, the threshold voltage shift depends on the pH value and could be explained by the history of the discharge (deprotonation) process of the film. In summary, it was possible to demonstrate that the effect of the solution pH variation would alter the concentration of one of the species involved in the reaction and result in a shift in the redox potential in the voltammetric and in the EGFET studies according to the Nernstian behavior.

4. Conclusion

The synthetic route to prepare WO_3, via sol-gel, was successful. From the diffractogram was possible to identify the formation of platelike particles, as well as, lamellar structure. The SEM confirmed the X-Ray driffraction data, indicating irregular stacking with rounded platelets with a length of around 10–20 nm and thickness less than 1.0 nm. Both the EGFET and voltammetric sensors exhibited the same electrochemical mechanism. Therefore, as a sensing film on a pH-EGFET configuration, as well as, voltammetry, the WO_3 material demonstrated a linear behavior and a high sensitivity (52 mV/pH and 60 mV/pH) for the pH range 2-12, close to the theoretical limit (59.2 mV/pH). Both techniques gave very close results. Therefore, these results suggest that the material is a good candidate as a pH sensor and may be even further employed as a biosensor for urea and glucose detection.

Acknowledgements

References

1. Song KS, Nakamura Y, Sasaki Y, Degawa M, Yang JH and Kawarada H. pH-sensitive diamond field-effect transistors (FETs) with directly aminated channel surface. *Analytica Chimica Acta*. 2006; 3-8:573-574.

2. Silva GM, Lemos SG, Pocrifka LA, Marreto PD, Rosario AV and Pereira EC. Development of low-cost metal oxide pH electrodes based on the polymeric precursor method. *Analytica Chimica Acta*. 2008; 616(1):36-41. http://dx.doi.org/10.1016/j.aca.2008.03.019. PMid:18471481

3. Bergveld P. Development of an ion-sensitive solid-state device for neurophysiological measurements. *IEEE Transactions on Biomedical Engineering*. 1970; 17:70-71. http://dx.doi.org/10.1109/TBME.1970.4502688.

4. Van Der Spiegel J, Lauks I, Chan P and Babic D. The extended gate chemically sensitive field effect transistor as multi-species microprobe. *Sensors and Actuators*. 1983; 4:291-298. http://dx.doi.org/10.1016/0250-6874(83)85035-5.

5. Chou JC, Chiang JL and Wu CL. pH and procaine sensing characteristics of extended-gate field-effect transistor based on indium tin oxide glass. *Japanese Journal of Applied Physics*. 2005; 44(7A):4838-4842. http://dx.doi.org/10.1143/JJAP.44.4838.

6. Silva GR, Matsubara EY, Corio P, Roselen JM and Mulato M. Carbon felt/carbon nanotubes/pani as ph sensor. *Materials Research Society Proceedings*. 2007; 1018:EE1410-1. http://dx.doi.org/10.1557/PROC-1018-EE14-10.

7. Batista PD, Mulato M, Graeff CFO, Fernandez FJR and Marques FD. SnO2 extended gate field-effect transistor as pH sensor. *Brazilian Journal of Physics*. 2006; 36(2a):478-481. http://dx.doi.org/10.1590/S0103-97332006000300066.

8. Batista PD and Mulato M. ZnO extended-gate field-effect transistors as *p*H sensors. *Applied Physics Letters*. 2005; 87(14):143508-143510. http://dx.doi.org/10.1063/1.2084319.

9. Guerra EM and Mulato M. Synthesis and characterization of vanadium oxide/hexadecylamine membrane and its application as pH-EGFET sensor. *Journal of Sol-Gel Science and Technology*. 2009; 52(3):315-320. http://dx.doi.org/10.1007/s10971-009-2062-7.

10. Guerra EM, Silva GR and Mulato M. Extended gate field effect transistor using V2O5 xerogel sensing membrane by sol-gel method. *Solid State Sciences*. 2009; 11(2):456-460. http://dx.doi.org/10.1016/j.solidstatesciences.2008.07.014.

11. Guidelli EJ, Guerra EM and Mulato M. Ion sensing properties of vanadium/tungsten mixed oxides. *Materials Chemistry and Physics*. 2011; 125(3):833-837. http://dx.doi.org/10.1016/j.matchemphys.2010.09.040.

12. Guidelli EJ, Guerra EM and Mulato M. Vanadium and titanium mixed oxide films: synthesis, characterization and application as ion sensor. *Journal of the Electrochemical Society*. 2012; 159(6):J217-J222. http://dx.doi.org/10.1149/2.053206jes.

13. Guidelli EJ, Guerra EM and Mulato M. E V2O5/WO3 mixed oxide films as pH-EGFET sensor: sequential re-usage and fabrication volume analysis. *ECS Journal Solid State Science and Technology*. 2012; 1(39):N39-N44. http://dx.doi.org/10.1149/2.007203jss.

14. Li X, Zhang Q, Miao W, Huang L, Zhang Z and Hua Z. Development of novel tungsten-doped high mobility transparent conductive In2O3 thin films. *Journal of Vacuum*

Science & Technology A: Vacuum, Surfaces, and Films. 2006; 24(5):1866-1869. http://dx.doi.org/10.1116/1.2333572.

15. Lee D, Nam K and Lee D. Effect of substrate on NO2-sensing properties of WO3 thin film gas sensors. *Thin Solid Films*. 2000; 375(1-2):142-146. http://dx.doi.org/10.1016/S0040-6090(00)01261-X.

16. Wang G, Ji Y, Huang X, Yang X, Gouma PI and Dudley M. Fabrication and characterization of polycrystalline WO3 nanofibers and their application for ammonia sensing. *The Journal of Physical Chemistry B*. 2006; 110(47):23777-23782. http://dx.doi.org/10.1021/jp0635819. PMid:17125339

17. Chemseddine A, Babonneau F and Livage J. Anisotropic WO. 3·nH2O layers deposited from gels. *Journal of Non-Crystalline Solids*. 1987; 91(2):271-278. http://dx.doi.org/10.1016/S0022-3093(87)80311-3.

18. Chien Y-S, Tsai W-L, Lee I-C, Chou J-C and Cheng H-C. A novel ph sensor of extended-gate field-effect transistors with laser-irradiated carbon-nanotube network. *IEEE Electron Device Letters*. 2012; 33(11):1622-1624. http://dx.doi.org/10.1109/LED.2012.2213794.

19. Temple-Boyer P, Launay J, Humenyuk I, Conto T, Martinez A, Beriet C, et al. Study of front-side connected chemical field effect transistor for water analysis. *Microelectronics and Reliability*. 2004; 44(3):443-447. http://dx.doi.org/10.1016/j.microrel.2003.10.001.

20. Walczak MM, Dryer DA, Jacobson DD, Foss MG and Flynn NT. pH-dependent redox couple: illustrating the nernst equation using cyclic voltammetry. *Journal of Chemical Education*. 1997; 74:1195-1197. http://dx.doi.org/10.1021/ed074p1195.

21. Yates DE, Levine S and Healey TW. Site-binding model of the electrical double layer at the oxide/water interface. *Journal of the Chemical Society, Faraday Transition 1: Physical Chemistry in Condensed Phases*. 1974; 70:1807-1818. http://dx.doi.org/10.1039/F19747001807.

22. Huang BR and Lin TC. Leaf-like carbon nanotube/nickel composite membrane extended-gate field-effect transistors as pH sensor. *Applied Physics Letters*. 2011; 99:023108. http://dx.doi.org/10.1063/1.3610554.

23. MacDonald DE, Rapuano BE and Schniepp HC. Surface oxide net charge of a titanium alloy: comparison between effects of treatment with heat or radiofrequency plasma glow discharge. *Colloids and Surfaces B: Biointerfaces*. 2011; 82(1):173-181. http://dx.doi.org/10.1016/j.colsurfb.2010.08.031. PMid:20880672